

Universal Approximation Theory: The basic theory for large language models

Wei Wang¹, Qing Li¹,

¹The Hong Kong Polytechnic University,
weiuat.wang@connect.polyu.hk, qing-prof.li@polyu.edu.hk

Abstract

Language models have emerged as a critical area of focus in artificial intelligence, particularly with the introduction of groundbreaking innovations like ChatGPT. Large-scale Transformer networks have quickly become the leading approach for advancing natural language processing algorithms. Built on the Transformer architecture, these models enable interactions that closely mimic human communication and, equipped with extensive knowledge, can even assist in guiding human tasks. Despite their impressive capabilities and growing complexity, a key question remains – the theoretical foundations of large language models (LLMs). What is it about the Transformer architecture that makes it so effective for powering intelligent language applications, such as translation and coding? What underlies LLMs’ ability for In-Context Learning (ICL)? How does the LoRA scheme enhance the fine-tuning of LLMs? And what supports the practicality of pruning LLMs? To address these critical questions and explore the technological strategies within LLMs, we leverage the Universal Approximation Theory (UAT) to offer a theoretical backdrop, shedding light on the mechanisms that underpin these advancements.

1 Introduction

In recent years, the rapid emergence of LLMs in the field of artificial intelligence has undoubtedly become one of the most notable advancements within the domain. The core allure of these models stems from their extraordinary capabilities in language processing. Language, as a unique crystallization of human intelligence, serves not only as the external reflection of thought but also as the bridge for communication, the cornerstone for the dissemination of knowledge, and the continuation of civilization, profoundly shaping the identity of humans as a unique species. Thus, endowing machines with the ability to understand and generate language marks a significant leap towards

the realization of true artificial intelligence. The emergence of models such as the ChatGPT (Radford and Narasimhan, 2018; Brown et al., 2020; Achiam et al., 2023), the Llama (Touvron et al., 2023), and the PaLM (Chowdhery et al., 2023) vividly demonstrates this point.

A distinctive feature of LLMs is their immense parameter size (Achiam et al., 2023; Touvron et al., 2023; Chowdhery et al., 2023; Chen et al., 2021; Zeng et al., 2022), often amounting to hundreds of billions or even trillions (for instance, GPT-3’s (Brown et al., 2020) 175 billion parameters and PaLM’s (Chowdhery et al., 2023) 540 billion parameters). This vast parameter scale lays the foundation for their exceptional language processing capabilities and enables them to exhibit almost human-like traits, such as ICL (Brown et al., 2020; Dong et al., 2022), instruction following (Sanh et al., 2021; Ouyang et al., 2022; Wei et al., 2021), and multi-step reasoning (Wei et al., 2022). Notably, these colossal models are predominantly trained by tech giants like Google and Microsoft using large-scale GPU clusters (Zhao et al., 2023), sparking a research fervor on how to efficiently fine-tune them with limited GPU resources. The advent of Lora (Hu et al., 2021) fine-tuning technology has provided an effective pathway for this, allowing for the fine-tuning of large models under resource constraints without the need to adjust all parameters of the original model comprehensively. Moreover, model pruning techniques (Sun et al., 2023; Ma et al., 2023) are crucial for deploying large models in resource-constrained environments, aiming to reduce the model size for operation on smaller devices. Faced with the challenge of processing long texts, such as generating summaries or answering questions based on extensive documents—which traditionally requires substantial computational resources—technologies like LongLora (Chen et al., 2023) have been developed to tackle the difficulties of processing long

contextual texts, further expanding the application boundaries of LLMs. Today, LLMs possess a diverse range of functionalities, from translation and text summarization to automatic code generation, demonstrating their versatility.

Despite LLMs being on a fast track of development towards higher intelligence and reliability, the theoretical foundation behind them remains largely unexplored, shrouded in clouds of uncertainty. The scientific community is actively seeking to uncover the inner mechanisms behind their powerful capabilities, including analyses of ICL mechanism (Xie et al., 2021; Min et al., 2022), among others. Against this backdrop, we establish the UAT (Cybenko, 2007; Hornik et al., 1989) as the mathematical essence of LLMs, and utilize the UAT lens to clarify pivotal technologies and phenomena within contemporary LLMs, aiming to illuminate this central theoretical conundrum from a fresh perspective. Our contributions are as follows:

- We prove that the Transformer is the tangible embodiment of UAT.
- We deliver a rigorous scientific explanation of Transformer-based LLMs through the UAT.
- We explain the characteristics of LLMs, such as ICL, instruction following, multi-step reasoning, and the technologies applied within LLMs like Lora, pruning, and LLMs’ strong generalization capabilities.
- We offer insights into the future development of LLMs.

Our article is structured as follows: In Section 2, we begin by introducing the UAT and propose that to demonstrate the Transformer’s adherence to UAT, it is necessary to show that both Linear and Multi-Head Attention (MHA) can be represented in the form of matrix-vector multiplication. In Section 3, we establish that the Transformer belongs to the category of UAT. Our proof strategy unfolds starting with Section 3.1, where we present the idea to express Linear and MHA as matrix-vector products. In Section 3.2, we detail the computational methods required for the proof. Sections 3.3 and 3.4 are dedicated to proving that both Linear and MHA can indeed be represented as matrix-vector operations. Further in Section 4, we leverage UAT to theoretically elucidate some fundamental issues (Generalization 4.1, ICL 4.2) and techniques (Pruning 4.3 and LoRA 4.4) associated with LLMs. Finally, we conclude with a summary of the existing

challenges and potential future developments for LLMs in Section 4.5.

2 The Universal Approximation Theory

Up to now, the UAT (Cybenko, 2007) is the most widely recognized fundamental theory in deep learning. However, this theorem is only applicable to the simplest form of neural networks, the multilayer perceptron (MLP) (Cybenko, 2007; Popescu et al., 2009). Due to the increased complexity of Transformer networks, they cannot be mathematically expressed in the same form as UAT. Thus, the theory has not yet been extended to Transformer networks. Our aim in this paper is to unify Transformer networks under the framework of UAT, thereby standardising their mathematical representation. Before unifying their mathematical forms, we provide a brief overview of the theorem, which was initially proposed by Cybenko (2007). This theorem encompasses numerous conclusions and proof details. Although it has been further developed, its fundamental mathematical form remains unchanged. Therefore, this paper explains the theory based on the UAT form presented by Cybenko (2007). Theorem 2 from Cybenko (2007) states that if σ is any continuous sigmoidal function, then finite sums of the following form:

$$G(\mathbf{x}) = \sum_{j=1}^N \alpha_j \sigma(\mathbf{W}_j^T \mathbf{x} + \theta_j) \quad (1)$$

is dense in $C(\mathbf{I}_n)$. Here, $\mathbf{W}_j \in \mathbb{R}^n$ and $\alpha_j, \theta \in \mathbb{R}$ are fixed. For any $f \in C(\mathbf{I}_n)$ and $\varepsilon > 0$, there exists a function $G(\mathbf{x})$:

$$|G(\mathbf{x}) - f(\mathbf{x})| < \varepsilon \quad \text{for all } \mathbf{x} \in \mathbf{I}_n. \quad (2)$$

This implies that, when N is sufficiently large, a neural network can approximate any continuous function on a closed interval. Hornik et al. (1989) further demonstrates that multilayer feedforward networks also conform to the UAT, capable of approximating arbitrary Borel measurable functions. Observing Equation (1), where the function $G(\mathbf{x})$ yields a scalar output in \mathbb{R} , the scenario expands naturally when $G(\mathbf{x})$ maps to \mathbb{R}^m , requiring the approximation in each dimension. It becomes evident that to accommodate this multidimensional output, a simple extension to Equation (1) suffices: the transformation matrix \mathbf{W}_j is revised to the space $\mathbb{R}^{n \times m}$, the bias term θ_j is recast as a vector in \mathbb{R}^m , and α_j is reshaped into a diagonal vector. Nevertheless, in these demonstrations, the theorem does

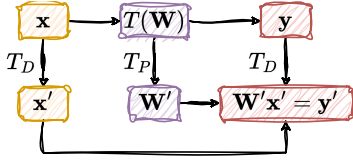


Figure 1: The transformation process of the Matrix-Vector Method.

not straightforwardly apply to Transformer architectures. However, if we succeed in reformulating both the Linear ($\mathbf{x}|\mathbf{W}$) and MHA ($\mathbf{x}|\mathbf{W}$) components into a unified representation, $\mathbf{W}'\mathbf{x}'$, where \mathbf{W} and \mathbf{x} represent the parameters and inputs for each component respectively, and \mathbf{W}' is derived from \mathbf{W} while \mathbf{x}' signifies a column vector (for details, refer to Section 3.1). It is easy to prove that multi-layer Transformer networks are concrete embodiments of UAT.

Consequently, our objective is to represent Linear and MHA architectures as a matrix-vector multiplication similar to Eq. (3). This approach offers two key benefits: Firstly, it allows for a fundamental mathematical investigation of deep learning models. Secondly, it provides a more intuitive and objective basis for comparing differences among various models. On this foundation, we propose to transform Linear and MHA into the matrix-vector format.

3 UAT for Transformer

In the previous section, we have outlined our fundamental goal to unify the Transformer model under the framework of UAT by converting Linear and MHA operations in the Transformer into matrix-vector forms. In this section, we will use the Matrix-Vector method to transform Transformer operations into matrix times vector forms.

3.1 Matrix-Vector Method

Before delving into transforming Linear and MHA into their matrix-vector format, we introduce the Matrix-Vector Method, which will subsequently be employed to cast both Linear and MHA operations into a unified matrix-vector format. This method constitutes a strategic realignment of input data and corresponding parameters of various transformations within the network, as illustrated in Figure 1. The underlying principle is as follows: both the input (\mathbf{x}) and output (\mathbf{y}) data are reconfigured uniformly through a transformation T_D into column vectors (\mathbf{x}' and \mathbf{y}'), while parameter tensor (\mathbf{W}) is reorganized into matrix form

(\mathbf{W}'). A critical requirement is that identical operations throughout the LLMs network adhere to the same restructuring scheme, thereby eliminating the need for additional transformations on intermediate feature data; they can directly be represented as column vectors. Additionally, by default, matrix variables in the original formulas are represented in bold, such as \mathbf{x} , and in the Matrix-Vector form, corresponding variables are denoted with a prime symbol ($'$) in the upper right corner, such as \mathbf{x}' . Elements within matrices are represented by corresponding lowercase letters with subscripts, for example, x_i . The Matrix-Vector Method can be succinctly encapsulated as follows:

$$\mathbf{y} = T(\mathbf{x}|\mathbf{W}) \rightarrow \mathbf{y}' = \mathbf{W}'\mathbf{x}' \quad (3)$$

It is obvious that T_D and T_P are not fixed, we could design various kinds of ways to do those. For convenience, we present a methodology tailored for Linear in Section 3.3 and an approach for MHA in Section 3.4, thereby illustrating the adaptability and application of the Matrix-Vector Method across different components of the Transformer architecture.

3.2 Diamond Matrix Multiplication

While our goal is to transform Linear and MHA modules into a matrix-vector format, this process is complex. In order to describe this transformation process clearly, we propose a new computational method called the Diamond Multiplication Method, denoted by the symbol \diamond .

$$\begin{pmatrix} w_{1,1} & w_{1,2} & \cdots & w_{1,n} \\ w_{2,1} & w_{2,2} & & w_{2,n} \\ \vdots & \vdots & \vdots & \vdots \\ w_{m,1} & w_{m,2} & & w_{m,n} \end{pmatrix} \diamond \begin{pmatrix} x_1 \\ x_2 \\ \vdots \\ x_m \end{pmatrix} \quad (4)$$

$$= \begin{pmatrix} w_{1,1}x_1 + w_{31} * x_2 + \cdots w_{m,1}x_m \\ w_{1,2}x_1 + w_{2,2}x_2 + \cdots w_{m,2}x_m \\ \vdots \\ w_{1,n}x_1 + w_{2,n}x_2 + \cdots w_{mn}x_m \end{pmatrix}$$

Let $\mathbf{W} \in \mathbb{R}^{(m,n)}$ and $\mathbf{x} \in \mathbb{R}^{(m,1)}$, the Diamond Matrix Multiplication is defined as $\mathbf{y} = \mathbf{W} \diamond \mathbf{x}$, where $\mathbf{y} \in \mathbb{R}^{(m,1)}$. The computation procedure involves element-wise multiplication and summation of corresponding elements from left to right across the columns of matrix \mathbf{W} with vector \mathbf{x} . The sum of the multiplication of the i th column of \mathbf{W} with \mathbf{x} is assigned as the i th element of \mathbf{y} . A detailed calculation process is provided in Eq. ((4)). The

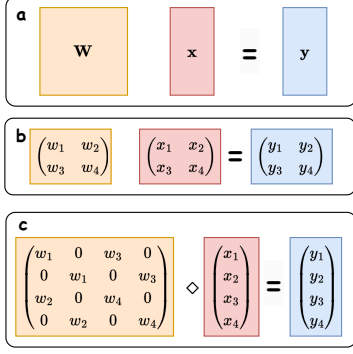


Figure 2: The process of converting a linear transformation into its corresponding matrix-vector representation. **a**: Depicts the general form of a linear transformation. **b**: Presents a straightforward example of a linear transformation. **c**: Demonstrates the transformation of the linear operation from **b** into the matrix-vector format.

computation process for $\mathbf{y} = \mathbf{x} \diamond \mathbf{W}$ is identical to that of $\mathbf{W} \diamond \mathbf{x}$, implying that $\mathbf{W} \diamond \mathbf{x} = \mathbf{x} \diamond \mathbf{W}$. However, it should be noted that the Diamond Matrix Multiplication does not possess the properties of associativity and distributivity.

Furthermore, based on its computation method, it can be inferred that the Diamond Matrix Multiplication is related to conventional matrix multiplication, specifically: $\mathbf{W} \diamond \mathbf{x} = \mathbf{W}^T \mathbf{x}$. Additionally, when \mathbf{W}_1 and \mathbf{W}_2 are square matrices, we can derive the following relationships: $\mathbf{W}_1 \diamond [\mathbf{x} \diamond \mathbf{W}_2] = \mathbf{W}_2^T \diamond \mathbf{W}_1 \diamond \mathbf{x}$ and $[\mathbf{W}_1 \diamond \mathbf{x}] \diamond \mathbf{W}_2 = \mathbf{W}_1^T \diamond \mathbf{W}_2 \diamond \mathbf{x}$. Detailed derivations can be found in [Appendix A](#).

3.3 Matrix-Vector Method for Linear

In this section, we present a way to transform Linear operation into matrix-vector format. Figure 2 illustrates this process: Figure 2.a shows the linear transformation of multi-channel input: $\mathbf{W}\mathbf{x} = \mathbf{y}$. Figure 2.b provides a specific example of Figure 2.a, Figure 2.c converts the linear transformation in Figure 2.b into the corresponding matrix-vector representation: $\mathbf{W}' \diamond \mathbf{x}' = \mathbf{y}'$. Thus, the linear transformation can be represented in matrix-vector form as follows:

$$\mathbf{x}_{i+1} = \mathbf{W}_i \mathbf{x}^i \rightarrow \mathbf{x}'_{i+1} = \mathbf{W}'_i \diamond \mathbf{x}'_i = (\mathbf{W}'_i)^T \mathbf{x}'_i \quad (5)$$

Here, $\mathbf{x}_i \in \mathbb{R}^{(N,M)}$ and $\mathbf{x}_{i+1} \in \mathbb{R}^{(N,M)}$ represent the input and output of layer i , respectively, while $\mathbf{W}_i \in \mathbb{R}^{(N,N)}$ represents the parameters of layer i . \mathbf{x}'_i , \mathbf{x}'_{i+1} , and \mathbf{W}'_i are generated based on \mathbf{x}^i , \mathbf{x}^{i+1} , and \mathbf{W}_i using the Matrix-Vector Method. The derivation of the general form can be found in [Appendix B.1](#).

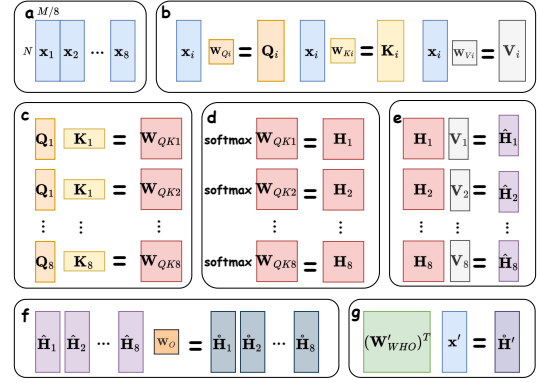


Figure 3: The Transformer process.

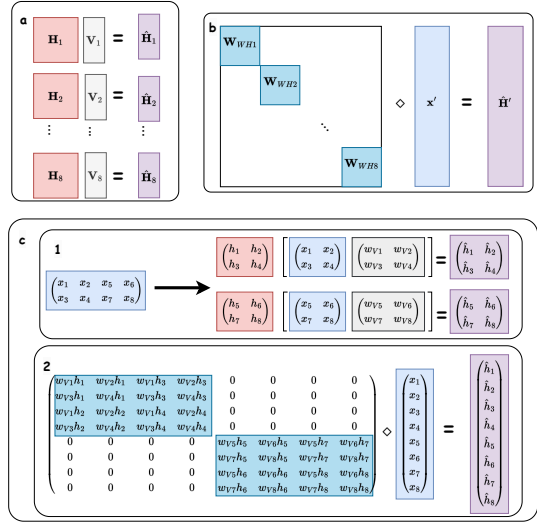


Figure 4: The process of transforming $\text{Concat}(\hat{\mathbf{H}}_1 \dots \hat{\mathbf{H}}_h)$ in the MHA into its corresponding matrix-vector form $\mathbf{W}'_{WH} \mathbf{x}' = \hat{\mathbf{H}}'$.

3.4 Matrix-Vector Method for MHA

We now employ the Matrix-Vector Method to elucidate the inner workings of the MHA. The mechanism is defined by the following equation:

$$\begin{aligned} \hat{\mathbf{H}} &= \text{MultiHead}(\mathbf{Q}, \mathbf{K}, \mathbf{V}) \\ &= \text{Concat}(\hat{\mathbf{H}}_1, \dots, \hat{\mathbf{H}}_h) \mathbf{W}_O \end{aligned} \quad (6)$$

$$\begin{aligned} \text{Attention}(\mathbf{x}_i \mathbf{W}_{Q_i} = \mathbf{Q}_i, \mathbf{x}_i \mathbf{W}_{K_i} = \mathbf{K}_i, \\ \mathbf{x}_i \mathbf{W}_{V_i} = \mathbf{V}_i) &= \text{softmax}\left(\frac{\mathbf{Q}_i \mathbf{K}_i^T}{\sqrt{M}}\right) \mathbf{V}_i \quad (7) \\ &= \mathbf{H}_i \mathbf{V}_i = \mathbf{H}_i [\mathbf{x}_i \mathbf{W}_{V_i}] = \hat{\mathbf{H}}_i \end{aligned}$$

Here, h represents the number of attention heads, and the input $\mathbf{x} \in \mathbb{R}^{(N,M)}$ is divided into $\mathbf{x}_1, \dots, \mathbf{x}_h$ based on h . The parameters \mathbf{W}_{Q_i} , \mathbf{W}_{K_i} , and \mathbf{W}_{V_i} correspond to \mathbf{x}_i . The whole process of MHA can be represented in Figure 3. Figure 3.a represents that the input \mathbf{x} is split into $\mathbf{x}_1 \dots \mathbf{x}_h$ based on the number of heads. Fig-

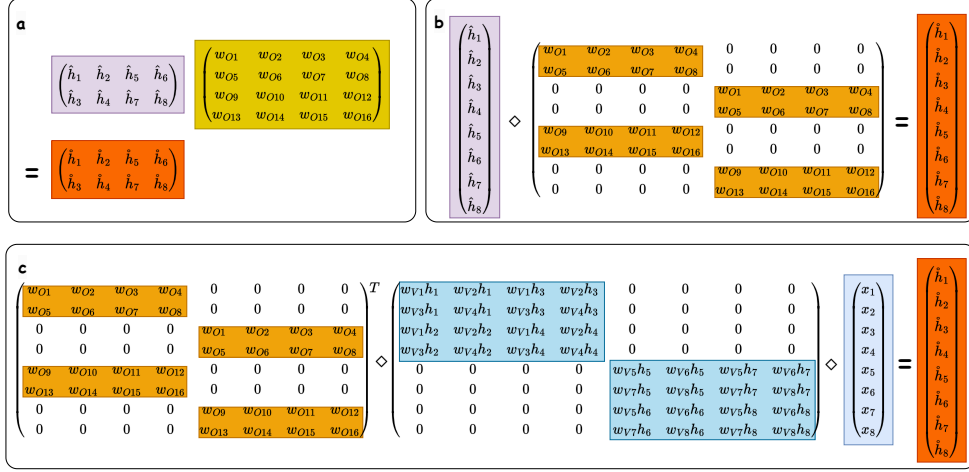


Figure 5: This diagram illustrates the process of transforming $\text{Concat}(\hat{\mathbf{H}}_1 \dots \hat{\mathbf{H}}) \mathbf{W}_O$ in the MHA into its corresponding matrix-vector form $\mathbf{W}'_{W_{HO}} \diamond \mathbf{x}' = \hat{\mathbf{H}}'$, different colors in the diagram correspond to different variables.

Figure 3.b represents $\mathbf{x}_i \mathbf{W}_{Q_i} = \mathbf{Q}_i$, $\mathbf{x}_i \mathbf{W}_{K_i} = \mathbf{K}_i$, $\mathbf{x}_i \mathbf{W}_{V_i} = \mathbf{V}_i$. Figure 3. c, d, e represent the process of $\text{softmax} \left(\frac{\mathbf{Q}_i \mathbf{K}_i^T}{\sqrt{M}} \right) \mathbf{V}_i$ and we omit \sqrt{M} .

Figure 3.f represents $\text{Concat}(\hat{\mathbf{H}}_1, \dots, \hat{\mathbf{H}}_h) \mathbf{W}_O$. Figure 3.g represents the whole process by a matrix multiplication of $(\mathbf{W}'_{HVO})^T \mathbf{x}' = \hat{\mathbf{H}}'$, where \mathbf{W}'_{HVO} is generated based $\mathbf{H}_1 \dots \mathbf{H}_8$, $\mathbf{W}_{V1} \dots \mathbf{W}_{V8}$ and \mathbf{W}_O . It means that we could represent the whole complex MHA into a matrix multiplication. Next, we give the proof of this process.

Our objective is to express the MHA as $(\mathbf{W}')^T_{HVO} \mathbf{x}' = \hat{\mathbf{H}}'$. Prior to transforming the MHA into the matrix-vector form, we need to conduct a comprehensive analysis and clearly define the research object. In Eq. (7), $\text{Concat}(\hat{\mathbf{H}}_1, \dots, \hat{\mathbf{H}}_h)$ describes an engineering process that requires mathematical representation. The learning process for the input \mathbf{x} primarily consists of two parts: $\mathbf{V}_1, \dots, \mathbf{V}_h$ and $\mathbf{H}_1, \dots, \mathbf{H}_h$. \mathbf{H}_i is derived based on the parameters \mathbf{W}_{Q_i} and \mathbf{W}_{K_i} , and can be directly regarded as parameters matrix now, a deep explanation is given in Section 3.5.

Figure 4.a represents the computation process of $\mathbf{H}_1 \mathbf{V}_1 = \hat{\mathbf{H}}_1, \dots, \mathbf{H}_h \mathbf{V}_h = \hat{\mathbf{H}}_h$, and in Figure 4.b, we convert it into the matrix-vector form $\mathbf{W}'_{WH} \diamond \mathbf{x}' = \hat{\mathbf{H}}'$, where \mathbf{W}'_{WH} is generated from $\mathbf{H}_1, \dots, \mathbf{H}_8$ and $\mathbf{W}_{V1}, \dots, \mathbf{W}_{V8}$. In Figure 4.c, we present a simple example, Figure 4.c.1 depicts $\mathbf{H}_i [\mathbf{x}_i \mathbf{W}_{V_i}]$, while Figure 4.c.2 represents the matrix-vector format of Figure 4.c.1. More details could be found in Appendix B.2.

Figure 5 illustrates the parameter transforma-

tion scenario after incorporating \mathbf{W}_O . Figure 5.a demonstrates an example of $\hat{\mathbf{H}} = \text{Concat}(\hat{\mathbf{H}}_1, \dots, \hat{\mathbf{H}}_h) \mathbf{W}_O$, while Figure 5.b rewrites Figure 5.a as $\mathbf{H}' \diamond \mathbf{W}'_O = \hat{\mathbf{H}}'$. Consequently, based on Figures 4 and 5, the entire MHA can be expressed as $\mathbf{W}'_{HVO} \diamond \mathbf{x}' = \hat{\mathbf{H}}'$, where $\mathbf{W}'_{HVO} = \mathbf{W}'_{WH} \diamond \mathbf{W}'_O$. So the whole MHA can be written as:

$$\hat{\mathbf{H}} = (\mathbf{W}'_{HVO})^T (\mathbf{x}_i)' \quad (8)$$

Here, $\mathbf{x}_i \in \mathbb{R}^{(NM,1)}$ and $\hat{\mathbf{H}} \in \mathbb{R}^{(NM,1)}$ are the input and output of i th layer, respectively, while $\mathbf{W}'_{HVO} \in \mathbb{R}^{(NM, NM)}$ denotes matrices generated in accordance with \mathbf{H} , \mathbf{W}_V and \mathbf{W}_O . In this manner, we have expressed MHA as a matrix-vector multiplication. This matrix multiplication representation provides a more concise way to express MHA mechanism.

Based on the derivations above and referring to Figure 4, we can gain a deeper understanding of the learning process in MHA. In particular, MHA can be regarded as a specialized form of linear transformation, which involves firstly dividing \mathbf{x} into $\mathbf{x}_1 \dots \mathbf{x}_h$ based on the number of heads, then transforming \mathbf{x}_i into \mathbf{x}'_i , and subsequently utilizing \mathbf{H}'_i , \mathbf{W}'_{V_i} , and \mathbf{W}'_{O_i} to generate the corresponding parameters \mathbf{W}'_{HVO_i} for \mathbf{x}'_i .

3.5 What makes Transformer to be the winner in LLMs?

The Transformer architecture is founded on two pivotal components: FFN and MHA. FFN is comprised of linear operations. In Sections 3.3 and 3.4, we have showcased the matrix-vector representations for both Linear and MHA. In this section, we

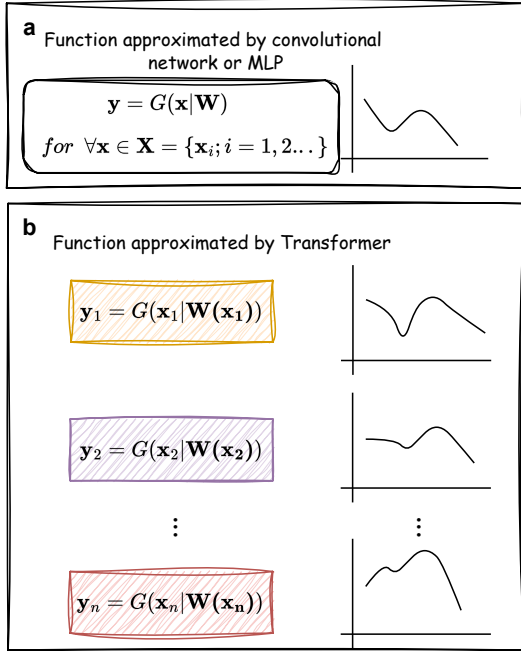


Figure 6: The approximation ways of the MLP (a) and Transformer (b) networks.

delve into why the Transformer has emerged as a key model in the domain of LLMs.

From a mathematical perspective, both the MLP and the Transformer serve as concrete implementations of the UAT. Through the matrix-vector approach, it is straightforward to demonstrate that convolutional networks also realize the UAT, thus sharing the same foundational mathematical principles. However, the question arises: Why does the Transformer hold a dominant position in LLMs? The answer lies in the ingenious design of the MHA. Unlike traditional linear operations, the parameters of MHA are dynamic, adjusting in response to the input data. While the UAT endows models with a powerful approximation capability, fixing the parameters in linear operations means that the function that an MLP can approximate remains unchanged, as illustrated in Figure 6.a. In contrast, the Transformer can adjust its parameters by \mathbf{H}'_i , based on the input. These parameters, \mathbf{H}'_i , should be regarded as being generated in response to the input, as depicted in Figure 6.b. This adaptability implies that the approximated function can vary with the input. This characteristic also explains the strong generalization capability of Transformer-based neural networks, as they can approximate different functions tailored to the requirements of various tasks, such as those needed for language translation versus mathematical problem-solving.

4 Discussion

Leveraging on our proof in the previous section that the Transformer is the tangible embodiment of UAT, in this section we address the following critical problems and explore the technical strategies of LLMs: Why does the Transformer architecture possess such power in enabling intelligent language models, such as translation and programming? What enables LLMs' capacity for ICL? How does the LoRA scheme effectively fine-tune LLMs? What justifies the feasibility of pruning LLMs?

4.1 The fundamental reason for the power of Transformers in LLMs

Theoretically, we have established that Transformer networks act as concrete implementations of the UAT, leveraging its potent capability to approximate any Borel measurable function, thus ensuring the high-dimensional function approximation advantage of models based on UAT. While UAT possesses immense function approximation abilities, it inherently lacks the capacity of approximating multiple functions simultaneously. However, language tasks are by nature diverse, potentially requiring the approximation of different functions based on the input. For instance, summarizing, translating, and continuing the same text content, the function space remains entirely the same except for minor variations in prompt words. Without the ability to dynamically approximate functions based on input, but merely fitting based on a general function trend, it would lead to approximating the same function, hence producing identical or similar output. Therefore, LLMs need to distinguish and adapt to these nearly identical functions, thereby dynamically generating response functions based on input. The MHA mechanism in Transformers provides LLMs with the capability to dynamically approximate relevant functions based on input. In particular, MHA mechanism allows for the dynamic adjustment of UAT's parameters according to the input, thereby laying the theoretical foundation for Transformer-based LLMs to simultaneously tackle multifaceted tasks such as translation, continuation, summarization, code generation, and solving mathematical problems.

4.2 What enables LLMs to possess ICL capability?

Contextual interaction, as the core capability of LLMs, permeates every phase from training and fine-tuning to prediction. ICL, multi-step reasoning, and instruction following are intuitive manifestations of this contextual interaction. Leveraging their context-sensitive interaction capabilities, LLMs can exhibit behaviors consistent with ICL, multi-step inference, and instruction following, which are tailored based on contextual cues. Furthermore, contemporary LLMs are evolving towards handling longer contexts; however, this advancement is accompanied by a dramatic increase in computational resource demands due to text expansion. A notable solution to this challenge is LongLoRA (Chen et al., 2023), which fundamentally also utilizes contextual interaction mechanisms to facilitate training on extended sequences.

So, how does this contextual interaction capability arise within LLMs? The formula $\dot{\mathbf{H}} = (\mathbf{W}'_{HVO})^T (\mathbf{x}^i)'$ in Figure 5 reveals this mode of contextual interaction. Since $(\mathbf{W}'_{HVO})^T$ represents a dense matrix (almost devoid of zero elements and whose internal elements are highly correlated), each element in $\dot{\mathbf{H}}$ encapsulates comprehensive information from both preceding and subsequent contexts. This learning of holistic contextual information constitutes the foundation of contextual interaction within LLMs.

4.3 What justifies the feasibility of pruning LLMs?

Due to the massive size of parameters in LLMs and the subsequent high demand for computational resources, pruning LLMs is pivotal for their deployment. A legitimate question to ask is why LLMs are amenable to pruning? The rationale lies in the presence of excessively low-weight parameters in certain layers of LLMs. To understand this, we can directly analyze it from the perspective of the formula underlying the UAT:

$$\left| \sum_{j=1}^N \alpha_j \sigma(\mathbf{W}_j^T \mathbf{x} + \theta_j) - f(\mathbf{x}) \right| < \varepsilon \quad (9)$$

for all $\mathbf{x} \in \mathbf{I}_n$. Let's assume $\Lambda = \{1, 2, \dots, N\}$, $\Lambda_1 \cup \Lambda_2 = \Lambda$, $\Lambda_1 \cap \Lambda_2 = \emptyset$ and $|\sum_{j \in \Lambda_1} \alpha_j \sigma(\mathbf{W}_j^T \mathbf{x} + \theta_j)| \rightarrow 0$. Then we have:

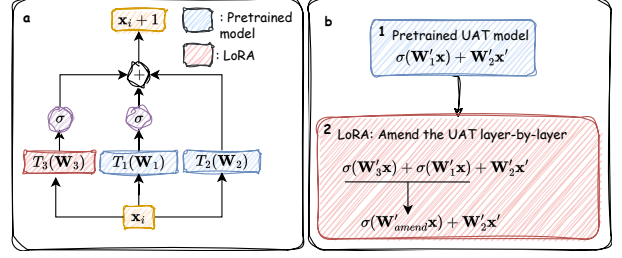


Figure 7: The LoRA process (a), and the operation from the perspective of UAT (b).

$$\begin{aligned} & \left| \sum_{j \in \Lambda_1} \alpha_j \sigma(\mathbf{W}_j^T \mathbf{x} + \theta_j) \right. \\ & \left. + \sum_{j \in \Lambda_2} \alpha_j \sigma(\mathbf{W}_j^T \mathbf{x} + \theta_j) - f(\mathbf{x}) \right| < \varepsilon \end{aligned} \quad (10)$$

Since $|\sum_{j \in \Lambda_1} \alpha_j \sigma(\mathbf{W}_j^T \mathbf{x} + \theta_j)| \rightarrow 0$, we have the following inequality:

$$\begin{aligned} & \left| \sum_{j \in \Lambda_1} \alpha_j \sigma(\mathbf{W}_j^T \mathbf{x} + \theta_j) - f(\mathbf{x}) \right| \\ & - \left| \sum_{j \in \Lambda_2} \alpha_j \sigma(\mathbf{W}_j^T \mathbf{x} + \theta_j) \right| < \varepsilon \end{aligned} \quad (11)$$

Therefore, we have:

$$\begin{aligned} & \left| \sum_{j=1}^{N_1} \alpha_j \sigma(\mathbf{W}_j^T \mathbf{x} + \theta_j) - f(\mathbf{x}) \right| \\ & < \varepsilon + \left| \sum_{j=1}^{N_2} \alpha_j \sigma(\mathbf{W}_j^T \mathbf{x} + \theta_j) \right| \end{aligned} \quad (12)$$

Hence, when parameters in certain layers are small enough, we can directly remove those layers since their impact on the final result is minimal.

4.4 How does the LoRA scheme effectively fine-tune LLMs?

Owing to the substantial computational resources required for training LLMs and their strong generalization capabilities, we believe the focus should be redirected towards efficiently leveraging pre-trained models. Repeatedly training models from scratch incurs considerable computational overhead, rendering the endeavor of repurposing well-trained models in novel tasks both practically valuable and resource-saving. A currently prominent solution addressing this issue is the LoRA methodology.

The LoRA scheme, illustrated in Figure 7.a, adopts a streamlined approach where T_i symbolically represents the transformations within the network. Given our prior establishment that these

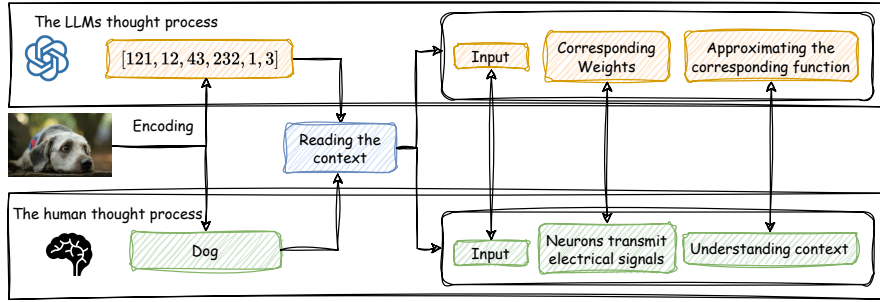


Figure 8: The comparison between Human and LLMs.

transformations can be cast into matrix-vector operations, from the perspective of the UAT, LoRA fundamentally constitutes a layer-wise fine-tuning tailored to specific task characteristics. This fine-tuning mechanism is depicted in Figures 7.b.1 and Figure 7.b.2, where \mathbf{W}'_{amend} signifies the parameters post-refinement, thereby embodying an adaptive calibration of the UAT’s underlying parameters to enhance task-specific performance.

4.5 Rethinking LLMs

The capabilities of LLMs have become so formidable that their language processing prowess is increasingly approaching human levels, prompting a core question: How do LLMs differ from humans in language processing? Figure 8 elucidates the contrast between the patterns employed by LLMs and humans. Both start with language encoding—humans through a character-based system and LLMs via numerical arrays—essentially, there is little difference at this foundational level. Given the polysemy of words, context determination is crucial: humans understand context through the activation and transmission of neurons in the human brain, while LLMs use patterns of parameter activation to approximate corresponding functions. Here, the activation of network parameters parallels the neural electrical signalling in the brain, and the approximation of functions corresponds to human comprehension of semantics. From this perspective, the difference in language processing between humans and LLMs seems minimal.

We posit that the main differences lie in human autonomy and multimodal perception. Human autonomy enables self-directed learning, allowing knowledge to be validated within real-world contexts and personal experiences, whereas LLMs are confined to function fitting based on the majority of corpora in their datasets, with the goal of optimizing loss minimization. Human multimodality encompasses interpreting the world through senses

such as vision, hearing, taste, and touch, infusing vocabulary with rich meanings, while LLMs are inherently adept to single-modality numerical representations.

Another significant issue in LLMs pertains to the segmentation of word embeddings within the MHA, as shown in Figure 4.a. Does this fragmentation still capture the full meaning of words comprehensively? If there are eight attention heads, does that mean a word has eight different encodings, suggesting a form of modality diversity, which then interacts through MHA to extract contextual insights? Furthermore, by considering LLMs as implementations of UAT, can we directly compute the weights necessary for function approximation from the data, thereby significantly reducing training overhead?

5 Conclusion

In this paper, we delve into the theoretical underpinnings of LLMs, demonstrating that contemporary LLMs, primarily constructed with Transformer architectures, embody concrete manifestations of the UAT. The remarkable generalization prowess exhibited by LLMs is attributed to their MHA modules, which enable the adaptation to and approximation of diverse functions based on the presented input data. Contextual interaction emerges as a paramount capability for LLMs, manifesting such abilities as ICL, instruction following, and contextual reasoning. These competencies are enabled by the Transformer’s innate capacity to learn from context.

Expanding upon this understanding, we have provided a rigorous theoretical grounding for key techniques employed in LLMs, including LoRA for efficient fine-tuning and pruning for model compression, elucidating their effectiveness through the lens of the UAT. By leveraging the theoretical framework provided by the UAT, not only can existing methodologies be explained but also avenues for the future evolution of LLMs are illuminated.

Limitation

Our work primarily delves into explaining a select few characteristics (ICL, Instruction following, and multi-step reasoning) and techniques (such as LoRA and Pruning) that we perceive as pivotal within current LLMs. While numerous advancements have been made to Transformer-based LLMs, their fundamental underpinnings largely align with the principles outlined herein. Nevertheless, due to space constraints, this paper does not aspire to exhaustively address every issue or attribute present across all LLMs. Instead, it focuses on elucidating those deemed most significant, thereby offering a concentrated insight into the core of LLMs. It is important to acknowledge that our scope, though carefully curated, is by no means exhaustive, and further exploration is warranted to gain a comprehensive understanding of the extensive landscape of LLMs enhancements and challenges.

References

- Josh Achiam, Steven Adler, Sandhini Agarwal, Lama Ahmad, Ilge Akkaya, Florencia Leoni Aleman, Diogo Almeida, Janko Altschmidt, Sam Altman, Shyamal Anadkat, et al. 2023. Gpt-4 technical report. *arXiv preprint arXiv:2303.08774*.
- Tom Brown, Benjamin Mann, Nick Ryder, Melanie Subbiah, Jared D Kaplan, Prafulla Dhariwal, Arvind Neelakantan, Pranav Shyam, Girish Sastry, Amanda Askell, et al. 2020. Language models are few-shot learners. *Advances in neural information processing systems*, 33:1877–1901.
- Mark Chen, Jerry Tworek, Heewoo Jun, Qiming Yuan, Henrique Ponde de Oliveira Pinto, Jared Kaplan, Harri Edwards, Yuri Burda, Nicholas Joseph, Greg Brockman, et al. 2021. Evaluating large language models trained on code. *arXiv preprint arXiv:2107.03374*.
- Yukang Chen, Shengju Qian, Haotian Tang, Xin Lai, Zhijian Liu, Song Han, and Jiaya Jia. 2023. [Longlora: Efficient fine-tuning of long-context large language models](#). *ArXiv*, abs/2309.12307.
- Aakanksha Chowdhery, Sharan Narang, Jacob Devlin, Maarten Bosma, Gaurav Mishra, Adam Roberts, Paul Barham, Hyung Won Chung, Charles Sutton, Sebastian Gehrmann, et al. 2023. Palm: Scaling language modeling with pathways. *Journal of Machine Learning Research*, 24(240):1–113.
- G. Cybenko. 2007. [Approximation by superpositions of a sigmoidal function](#). *Mathematics of Control, Signals, and Systems*, page 303–314.
- Qingxiu Dong, Lei Li, Damai Dai, Ce Zheng, Zhiyong Wu, Baobao Chang, Xu Sun, Jingjing Xu, and Zhifang Sui. 2022. A survey on in-context learning. *arXiv preprint arXiv:2301.00234*.
- Kurt Hornik, Maxwell B. Stinchcombe, and Halbert L. White. 1989. [Multilayer feedforward networks are universal approximators](#). *Neural Networks*, 2:359–366.
- Edward J Hu, Yelong Shen, Phillip Wallis, Zeyuan Allen-Zhu, Yuanzhi Li, Shean Wang, Lu Wang, and Weizhu Chen. 2021. Lora: Low-rank adaptation of large language models. *arXiv preprint arXiv:2106.09685*.
- Xinyin Ma, Gongfan Fang, and Xinchao Wang. 2023. Llm-pruner: On the structural pruning of large language models. *Advances in neural information processing systems*, 36:21702–21720.
- Sewon Min, Xinxu Lyu, Ari Holtzman, Mikel Artetxe, Mike Lewis, Hannaneh Hajishirzi, and Luke Zettlemoyer. 2022. [Rethinking the role of demonstrations: What makes in-context learning work?](#) In *Proceedings of the 2022 Conference on Empirical Methods in Natural Language Processing*, pages 11048–11064, Abu Dhabi, United Arab Emirates. Association for Computational Linguistics.
- Long Ouyang, Jeffrey Wu, Xu Jiang, Diogo Almeida, Carroll Wainwright, Pamela Mishkin, Chong Zhang, Sandhini Agarwal, Katarina Slama, Alex Ray, et al. 2022. Training language models to follow instructions with human feedback. *Advances in neural information processing systems*, 35:27730–27744.
- Marius-Constantin Popescu, Valentina E Balas, Liliana Perescu-Popescu, and Nikos Mastorakis. 2009. Multilayer perceptron and neural networks. *WSEAS Transactions on Circuits and Systems*, 8(7):579–588.
- Alec Radford and Karthik Narasimhan. 2018. [Improving language understanding by generative pre-training](#).
- Victor Sanh, Albert Webson, Colin Raffel, Stephen H Bach, Lintang Sutawika, Zaid Alyafeai, Antoine Chaffin, Arnaud Stiegler, Teven Le Scao, Arun Raja, et al. 2021. Multitask prompted training enables zero-shot task generalization. *arXiv preprint arXiv:2110.08207*.
- Mingjie Sun, Zhuang Liu, Anna Bair, and J Zico Kolter. 2023. A simple and effective pruning approach for large language models. *arXiv preprint arXiv:2306.11695*.
- Hugo Touvron, Thibaut Lavril, Gautier Izacard, Xavier Martinet, Marie-Anne Lachaux, Timothée Lacroix, Baptiste Rozière, Naman Goyal, Eric Hambro, Faisal Azhar, et al. 2023. Llama: Open and efficient foundation language models. *arXiv preprint arXiv:2302.13971*.
- Jason Wei, Maarten Bosma, Vincent Y Zhao, Kelvin Guu, Adams Wei Yu, Brian Lester, Nan

Du, Andrew M Dai, and Quoc V Le. 2021. Fine-tuned language models are zero-shot learners. *arXiv preprint arXiv:2109.01652*.

Jason Wei, Xuezhi Wang, Dale Schuurmans, Maarten Bosma, Fei Xia, Ed Chi, Quoc V Le, Denny Zhou, et al. 2022. Chain-of-thought prompting elicits reasoning in large language models. *Advances in neural information processing systems*, 35:24824–24837.

Sang Michael Xie, Aditi Raghunathan, Percy Liang, and Tengyu Ma. 2021. [An explanation of in-context learning as implicit bayesian inference](#). *ArXiv*, abs/2111.02080.

Aohan Zeng, Xiao Liu, Zhengxiao Du, Zihan Wang, Hanyu Lai, Ming Ding, Zhuoyi Yang, Yifan Xu, Wendi Zheng, Xiao Xia, et al. 2022. Glm-130b: An open bilingual pre-trained model. *arXiv preprint arXiv:2210.02414*.

Wayne Xin Zhao, Kun Zhou, Junyi Li, Tianyi Tang, Xiaolei Wang, Yupeng Hou, Yingqian Min, Beichen Zhang, Junjie Zhang, Zican Dong, et al. 2023. A survey of large language models. *arXiv preprint arXiv:2303.18223*.

A The Property of Diamond

There are two properties are always used: $\mathbf{W}_1 \diamond [\mathbf{x} \diamond \mathbf{W}_2] = \mathbf{W}_2^T \diamond \mathbf{W}_1 \diamond \mathbf{x} = \mathbf{W}_{12}$ and $[\mathbf{W}_1 \diamond \mathbf{x}] \diamond \mathbf{W}_2 = \mathbf{W}_1^T \diamond \mathbf{W}_2 \diamond \mathbf{x}$, where $\mathbf{W}_{12} = \mathbf{W}_1^T \mathbf{W}_2^T$. They are proved in Eq. (13) and (14).

$$\begin{aligned}
& \mathbf{W}_1 \diamond [\mathbf{x} \diamond \mathbf{W}_2] \\
&= \mathbf{W}_1 \diamond [\mathbf{W}_2^T \mathbf{x}] \\
&= \mathbf{W}_1^T [\mathbf{W}_2^T \mathbf{x}] \\
&= \mathbf{W}_1^T \mathbf{W}_2^T \mathbf{x} = \mathbf{W}_{12} \mathbf{x} \\
&= (\mathbf{W}_1^T \mathbf{W}_2^T)^T \diamond \mathbf{x} \\
&= (\mathbf{W}_2 \mathbf{W}_1) \diamond \mathbf{x} \\
&= \mathbf{W}_2 \diamond \mathbf{W}_1 \diamond \mathbf{x} \\
&= \mathbf{W}_2^T \diamond \mathbf{W}_1 \diamond \mathbf{x}
\end{aligned} \tag{13}$$

$$\begin{aligned}
& [\mathbf{W}_1 \diamond \mathbf{x}] \diamond \mathbf{W}_2 \\
&= [\mathbf{W}_1^T \mathbf{x}] \diamond \mathbf{W}_2 \\
&= \mathbf{W}_2^T [\mathbf{W}_1^T \mathbf{x}] \\
&= [\mathbf{W}_2^T \mathbf{W}_1^T]^T \diamond \mathbf{x} \\
&= [\mathbf{W}_1 \mathbf{W}_2] \diamond \mathbf{x} \\
&= \mathbf{W}_1 \diamond \mathbf{W}_2 \diamond \mathbf{x} \\
&= \mathbf{W}_1^T \diamond \mathbf{W}_2 \diamond \mathbf{x}
\end{aligned} \tag{14}$$

B The Matrix-Vector Form of Linear and MHA

In this section, we will present the transformation process Linear and MHA into their corresponding matrix-vector forms.

B.1 The Matrix-Vector Form of Linear

Eq. ((15)) gives the transformation method for Linear, it can be deduced that if the input data matrix has dimensions (N, M) and the parameter matrix has dimensions (N, N) , the sparsity of the parameter matrix corresponding to the Linear operation is $1/M$.

B.2 The Matrix-Vector Form of MHA

Figure 1.a represents the computation process of obtaining \mathbf{W}_{QKi} in the attention mechanism, while Figure 1.b computes $\mathbf{H}_1, \dots, \mathbf{H}_8$ through the *softmax* operation. Figure 1.c and Figure 1.e illustrates the process of converting $\text{Concat}(\hat{\mathbf{H}}_1 \mathbf{V}_1, \dots, \hat{\mathbf{H}}_h \mathbf{V}_h)$ into the matrix-vector form $\mathbf{W}'_{WH} \diamond \mathbf{x}' = \hat{\mathbf{H}}'$, where \mathbf{W}'_{WH} is generated from $\mathbf{H}_1, \dots, \mathbf{H}_8$ and $\mathbf{W}_{V1}, \dots, \mathbf{W}_{V8}$. Figure 1.c computes $\hat{\mathbf{H}}_i[\mathbf{x}_i \mathbf{W}_{Vi}]$. In Figure 1.d,

we provide a simple example demonstrating the conversion of $\hat{\mathbf{H}}_i[\mathbf{x}_i \mathbf{W}_{Vi}]$ into $\mathbf{W}'_{WHi} \mathbf{x}'_i$. This process is divided into four parts: Figure 1.d.1 represents the general form of $\hat{\mathbf{H}}_i[\mathbf{x}_i \mathbf{W}_{Vi}]$, while Figure 1.d.2 serves as a simple example of Figure 1.d.1. Figure 1.d.3 first rewrites Figure 1.d.2 using diamond multiplication as $\hat{\mathbf{H}}'_i \diamond [\mathbf{x}'_i \diamond \mathbf{W}'_{Vi}]$, and then utilizes the property of diamond multiplication to express it as $[\mathbf{W}'_{Vi} \hat{\mathbf{H}}'_i] \mathbf{x}'_i$. Finally, Figure 1.d.4 is obtained as $\mathbf{W}'_{WHi} \mathbf{x}'_i$. It can be observed that \mathbf{W}'_{WHi} is a dense matrix. In Figure 1.e, we present the conversion of the entire $\mathbf{H}_1[\mathbf{x}_1 \mathbf{W}_{V1}] \dots \mathbf{H}_8[\mathbf{x}_8 \mathbf{W}_{V8}]$ into the matrix-vector form $\mathbf{W}'_{WH} \mathbf{x}'$. In Figure 1.f, we present a simple example of Figure 1.e. Figure 1.f.1 depicts $\mathbf{H}_i[\mathbf{x}_i \mathbf{W}_{Vi}]$, while Figure 1.f.2 represents the Matrix-vector format of Figure 1.f.1.

$$\begin{aligned}
& \begin{pmatrix} w_{1,1} & w_{1,2} & \cdots & w_{1,n} \\ w_{2,1} & w_{2,2} & \cdots & w_{2,n} \\ \vdots & \vdots & \vdots & \vdots \\ w_{n,1} & w_{n,2} & \cdots & w_{n,n} \end{pmatrix} \begin{pmatrix} x_{1,1} & x_{1,2} & \cdots & x_{1,m} \\ x_{2,1} & x_{2,2} & \cdots & x_{2,m} \\ \vdots & \vdots & \vdots & \vdots \\ x_{n,1} & x_{n,2} & \cdots & x_{n,m} \end{pmatrix} = \begin{pmatrix} y_{1,1} & y_{1,2} & \cdots & y_{1,m} \\ y_{2,1} & y_{2,2} & \cdots & y_{2,m} \\ \vdots & \vdots & \vdots & \vdots \\ y_{n,1} & y_{n,2} & \cdots & y_{n,m} \end{pmatrix} \\
\rightarrow & \begin{pmatrix} w_{1,1} & 0 & \cdots \\ 0 & w_{1,1} & \cdots \\ \vdots & \vdots & \cdots \\ 0 & 0 & \cdots \\ w_{1,2} & 0 & \cdots \\ 0 & w_{1,2} & \cdots \\ \vdots & \vdots & \cdots \\ 0 & 0 & \cdots \\ \vdots & \vdots & \cdots \\ w_{1,n} & 0 & \cdots \\ 0 & w_{1,n} & \cdots \\ \vdots & \vdots & \cdots \\ 0 & 0 & \cdots \end{pmatrix} \diamond \begin{pmatrix} x_{1,1} \\ x_{1,2} \\ \vdots \\ x_{1,m} \\ x_{2,1} \\ x_{2,2} \\ \vdots \\ x_{2,m} \\ \vdots \\ x_{n,1} \\ x_{n,2} \\ \vdots \\ x_{n,m} \end{pmatrix} = \begin{pmatrix} y_{1,1} \\ y_{1,2} \\ \vdots \\ y_{1,m} \\ y_{2,1} \\ y_{2,2} \\ \vdots \\ y_{2,m} \\ \vdots \\ y_{n,1} \\ y_{n,2} \\ \vdots \\ y_{n,m} \end{pmatrix}
\end{aligned} \tag{15}$$
